

Optimal third-kind Chebyshev collocation algorithm for solving beam-type micro- and nanoscale BVPs

Youssri Hassan Youssri^{†*}, Ahmed Gamal Atta[‡]

[†]Department of Mathematics, Faculty of Science, Cairo University, Giza 12613, Egypt

[‡]Department of Mathematics, Faculty of Education, Ain Shams University, Roxy, Cairo 11341, Egypt

Email(s): youssri@cu.edu.eg, ahmed_gamal@edu.asu.edu.eg

Abstract. In this paper, we develop a numerical scheme for solving nonlinear boundary value problems (BVPs) arising in cantilever-type micro-electromechanical (MEMS) and nano-electromechanical (NEMS) systems. The method is based on a novel third-kind Chebyshev collocation approach. We derive an operational matrix of derivatives using shifted third-kind Chebyshev polynomials, which enables efficient spectral approximations of the governing equations. Numerical experiments confirm the accuracy and efficiency of the proposed method in handling the nonlinearities present in MEMS/NEMS actuator models.

Keywords: Third-kind Chebyshev polynomials, collocation method, MEMS/NEMS actuators, nonlinear boundary value problems.

AMS Subject Classification 2010: 65L10, 41A10, 70K50, 74H15.

1 Introduction

The applications of micro- and nano-electromechanical systems (MEMS/NEMS) in biomedical devices, sensors, and actuators have drawn a lot of interest. A conducting electrode hanging over a conductive substrate makes up beam-type electrostatic actuators, a key part of MEMS/NEMS. The movable electrode deflects when a voltage is supplied, creating a nonlinear electrostatic force that controls its dynamics. Designing dependable devices requires an understanding of the pull-in instability of such actuators [13, 18].

Because of their excellent accuracy and efficiency in solving differential equations, spectral methods have attracted a lot of attention [10, 25]. These techniques can be broadly divided into three categories: tau, Galerkin, and collocation techniques. The type of difficulty determines which option is the best. Galerkin methods assist theoretical analysis and offer ideal error estimates, whereas collocation methods are especially useful for nonlinear problems or equations with complex coefficients [27]. In contrast, the tau method works well for situations with complex or nonlinear boundary conditions, where collocation can become computationally costly and the Galerkin approach may not be appropriate [12]. For more studies, see [2–6, 19].

In physics and engineering, the collocation method is frequently employed to solve differential equations effectively. By choosing appropriate basis functions, it offers a spectral approximation with excellent precision. With their high accuracy and computational efficiency, collocation methods have become effective numerical techniques

*Corresponding author

Received: 17 May 2025 / Revised: 5 June 2025 / Accepted: 10 June 2025
DOI: 10.22124/JMM.2025.30690.2747

for resolving a variety of scientific and engineering problems [20]. As it can effectively handle complex boundary conditions, the variational collocation approach has garnered a lot of interest among these techniques [17]. Furthermore, high-order collocation techniques have shown superior convergence qualities in a large number of applications to differential equations with random inputs [28].

Recent advances in collocation methods have further expanded their applicability, explicit collocation techniques based on third-kind Chebyshev polynomials have demonstrated exceptional efficiency in solving nonlinear fractional Duffing equations in the setting of fractional differential equations [35]. Furthermore, the adaptability and resilience of spectral collocation approaches leveraging Chebyshev polynomials have been demonstrated by their effective application to a variety of models, such as fractional Bratu-type equations and interacting biological species [8, 26]. Yassin et al. [29] used shifted Schrder polynomials to solve the fractional Bagley-Torvik equation. These advancements highlight the increasing significance of collocation techniques in numerical analysis as well as their capacity to handle mathematical models that are getting more and more complicated like fractional integro-differential equations [31]. Youssri and Atta handled the model that simulated the human corneal shape in [33].

In numerical analysis, Chebyshev polynomials are essential, especially for approximating functions and solving differential equations [9, 14, 23]. Because of their characteristics, they are very useful in spectral and interpolation techniques, and they have made important contributions to theoretical and applied mathematics [21]. Their applicability in numerical algorithms has been further increased by the use of Chebyshev interpolation in rigorous computing [11]. Furthermore, Chebyshev polynomial approximations have proven their applicability in the physical sciences and engineering by successfully solving dynamical response problems in random systems [16]. Spectral methods have been widely used for solving fractional differential equations. Youssri and Atta [32] applied a modal spectral Tchebyshev Petrov–Galerkin approach to the time-fractional nonlinear Burgers equation, while Youssri et al. [30] developed a Chebyshev Petrov–Galerkin procedure for the time-fractional heat equation with nonlocal conditions, Moustafa et al. [22] introduced an explicit Chebyshev Petrov–Galerkin scheme for the time-fractional Euler–Bernoulli beam equation. Atta and Youssri [7] employed a shifted second-kind Chebyshev spectral collocation method for the time-fractional KdV-Burgers equation, Youssri and Atta [34] extended the Chebyshev Petrov–Galerkin method to nonlinear time-fractional integro-differential equations with a mildly singular kernel.

The main contribution of this work is the development of a novel third-kind Chebyshev collocation method for solving nonlinear MEMS/NEMS actuator models. The key contributions are:

- Construction of an operational matrix for derivatives, transforming the governing equations into a system of algebraic equations.
- Efficient solution of the resulting system of algebraic equations.
- High accuracy of the proposed method compared to the existing numerical schemes.

The organization of this paper is as follows: Section 2 presents the properties of the third-kind Chebyshev polynomials. Section 3 details the collocation algorithm and choice of basis functions. The error analysis for the proposed shifted third-kind Chebyshev expansion is studied in Section 4. Section 5 provides numerical results and comparisons with existing methods. Finally, Section 6 concludes the paper with remarks on the significance of the findings and potential future extensions.

2 Properties of third-kind Chebyshev polynomials

In this section, we provide the necessary definitions and mathematical preliminaries that will be used throughout this paper.

2.1 Third-kind Chebyshev polynomials

The third-kind Chebyshev polynomials are a sequence of polynomials defined by the following trigonometric form:

$$V_n(x) = \sqrt{\frac{1 + \cos((1 + 2n)\theta)}{1 + \cos \theta}}, \quad x = \cos \theta, \quad x \in [-1, 1], \quad n \in \mathbb{N} \cup \{0\}.$$

They satisfy the following second-order Sturm-Liouville differential equation:

$$(1 - x^2)u'' + (1 - 2x)u' + (n + n^2)u = 0.$$

These polynomials can also be generated via the Rodrigues' formula:

$$V_n(x) = \left((-1)^n \prod_{k=1}^n \frac{2k}{2k-1} \right) \frac{1}{w} D^n [(1 - x^2)^n w],$$

where

$$w \equiv w(x) = \sqrt{\frac{1+x}{1-x}}.$$

Additionally, they can be generated by the following second-order recurrence relation:

$$V_n(x) = 2xV_{n-1}(x) - V_{n-2}(x), \quad n \geq 2,$$

with the initial conditions:

$$V_0(x) = 1, \quad V_1(x) = 2x - 1.$$

These polynomials satisfy the following orthogonality relation:

$$\int_{-1}^1 V_r(x)V_s(x)w dx = \int_0^\pi (\cos((r-s)\theta) - \cos((r+s+1)\theta))d\theta = \pi\delta_{r,s}, \quad \forall r,s \in \mathbb{N} \cup \{0\}.$$

2.2 Shifted third-kind Chebyshev polynomials

The interval $[0, 1]$ is generally more convenient to work with than $[-1, 1]$. To transform the independent variable $x \in [-1, 1]$ into a variable x in $[0, 1]$, we apply the transformation $x \Rightarrow 2x - 1$. This results in the shifted third-kind Chebyshev polynomials $\bar{V}_k(x)$ of degree k in x on $[0, 1]$, given by $\bar{V}_k(x) = V_k(2x - 1)$. These polynomials are orthogonal over the interval $[0, 1]$ with the following inner product:

$$\langle \bar{V}_r, \bar{V}_s \rangle_{\bar{w}(x)} = \int_0^1 \bar{V}_r \bar{V}_s \sqrt{\frac{x}{1-x}} dx = \frac{\pi}{2} \delta_{r,s}. \tag{1}$$

The polynomials $\bar{V}_k(x)$ can also be generated using the recurrence relation [24]:

$$\bar{V}_k(x) = 2(2x - 1)\bar{V}_{k-1}(x) - \bar{V}_{k-2}(x), \quad k = 2, 3, \dots, \quad \text{with } \bar{V}_0(x) = 1, \bar{V}_1(x) = 4x - 3. \tag{2}$$

The explicit power and inversion formulae for the shifted third-kind Chebyshev polynomials are given by:

$$\bar{V}_r(x) = \sum_{i=0}^r A_{i,r} x^i, \tag{3}$$

where, $A_{i,r} = \frac{2^{2i}(-1)^{r+i}(2r+1)(r+i)!}{(2i+1)!(r-i)!}$

$$x^s = \frac{(2s+1)!}{2^{2s}} \sum_{\ell=0}^s \frac{1}{(s-\ell)!(\ell+s+1)!} \bar{V}_\ell(x). \tag{4}$$

Theorem 1. ([1]) The following formula for the r^{th} -order derivative of \bar{V}_k is correct for all $r \geq k$

$$D^r \bar{V}_k(x) = \frac{2^{2r}}{(r-1)!} \sum_{\ell=0}^{\lfloor (k-r)/2 \rfloor} \frac{(k-\ell)!(\ell+r-1)!}{\ell!(k-\ell-r)!} \bar{V}_{k-2\ell-r}(x) \\ + \frac{2^{2r}}{(r-1)!} \sum_{\ell=0}^{\lfloor (k-r-1)/2 \rfloor} \frac{(k-\ell-1)!(\ell+r)!}{\ell!(k-\ell-r)!} \bar{V}_{k-2\ell-r-1}(x).$$

Lemma 1. In Theorem 1, for $r = 4$ after fixing the indices, we have

$$D^4 \bar{V}_i(x) = \frac{128}{3} \sum_{\ell=0}^{i-4} \xi_{\ell,i} \bar{V}_{\ell}(x),$$

where

$$\xi_{\ell,k} = \begin{cases} \left(\frac{\ell-k-2}{2}\right)_3 \cdot \left(\frac{\ell+k-2}{2}\right)_4 & \text{if } k-\ell \text{ is even,} \\ \left(\frac{\ell-k-3}{2}\right)_4 \cdot \left(\frac{\ell+k-1}{2}\right)_3 & \text{if } k-\ell \text{ is odd,} \end{cases}$$

and $(y)_m = \frac{\Gamma(y+m)}{\Gamma(y)}$ is the Pochhammer symbol.

3 Collocation algorithm for the two Cantilever NEMS models

We consider the nonlinear BVP for the cantilever NEMS with negative-power nonlinearities

$$\frac{d^4 y}{dx^4} + \frac{\alpha_K}{y^K} + \frac{\mu}{y^2} + \frac{\gamma}{y} = 0, \quad 0 < x < 1, \quad K = 3, 4, \quad (5)$$

for Cantilever NEMS model subject to

$$y(0) = 1, \quad y'(0) = 0, \quad y''(1) = 0, \quad y'''(1) = 0, \quad (6)$$

while for double Cantilever NEMS model subject to

$$y(0) = 1, \quad y'(0) = 0, \quad y(1) = 1, \quad y'(1) = 0. \quad (7)$$

Using the substitution $u(x) = y(x) - 1$, transform the model (5) together with the conditions (6) and (7) to the following updated model:

$$\frac{d^4 u}{dx^4} + \frac{\alpha_K}{(1+u)^K} + \frac{\mu}{(1+u)^2} + \frac{\gamma}{1+u} = 0, \quad 0 < x < 1, \quad K = 3, 4, \quad (8)$$

for Cantilever NEMS model subject to

$$u(0) = u'(0) = 0, \quad u''(1) = 0, \quad u'''(1) = 0, \quad (9)$$

while for double Cantilever NEMS model subject to

$$u(0) = u'(0) = 0, \quad u(1) = 0, \quad u'(1) = 0. \quad (10)$$

3.1 Choice of the basis functions

Due to the presence of the two homogenous initial conditions $u(0) = u'(0) = 0$ in the two models of interest, we suggest the following basis functions

$$\rho_i(x) = x^2 \bar{V}_i(x), \quad i = 0, 1, \dots, n.$$

It is crystal clear that $\rho_i(0) = \rho'_i(0) = 0$ for every i .

Remark 1. Based on the orthogonality relation (1), one has

$$\int_0^1 \rho_r(x) \rho_s(x) w(x) dx = \frac{\pi}{2} \delta_{r,s}, \tag{11}$$

where $w(x) = \frac{1}{x^4} \sqrt{\frac{x}{1-x}}$.

Proof. Based on the definition of $\rho_i(x) = x^2 \bar{V}_i(x)$ along with the orthogonality relation (1), we can write

$$\frac{\pi}{2} \delta_{r,s} = \int_0^1 \bar{V}_r(x) \bar{V}_s(x) \sqrt{\frac{x}{1-x}} dx = \int_0^1 x^2 \bar{V}_r(x) x^2 \bar{V}_s(x) \frac{1}{x^4} \sqrt{\frac{x}{1-x}} dx = \int_0^1 \rho_r(x) \rho_s(x) w(x) dx, \tag{12}$$

where $w(x) = \frac{1}{x^4} \sqrt{\frac{x}{1-x}}$. □

Lemma 2. The following representation of $\rho_i(x)$ is valid:

$$\rho_i(x) = \frac{1}{16} [\bar{V}_{i-2}(x) + 4\bar{V}_{i-1}(x) + 6\bar{V}_i(x) + 4\bar{V}_{i+1}(x) + \bar{V}_{i+2}(x)].$$

Proof. In relation (2), we isolate $x\bar{V}_{k-1}(x)$ to obtain the following expression:

$$x\bar{V}_{k-1}(x) = \frac{\bar{V}_k(x) + 2\bar{V}_{k-1}(x) + \bar{V}_{k-2}(x)}{4}.$$

By applying this moment formula twice, the proof is then completed. □

Theorem 2. We have

$$\frac{d^4 \rho_i(x)}{dx^4} = \sum_{\ell=0}^{i-2} \eta_{\ell,i} \bar{V}_\ell(x),$$

where

$$\eta_{\ell,i} = \frac{8}{3} \begin{cases} \xi_{\ell,i-2} + 4\xi_{\ell,i-1} + 6\xi_{\ell,i} + 4\xi_{\ell,i+1} + \xi_{\ell,i+2} & \text{if } 0 \leq \ell \leq i-6, \\ 4\xi_{\ell,i-1} + 6\xi_{\ell,i} + 4\xi_{\ell,i+1} + \xi_{\ell,i+2} & \text{if } \ell = i-5, \\ 6\xi_{\ell,i} + 4\xi_{\ell,i+1} + \xi_{\ell,i+2} & \text{if } \ell = i-4, \\ 4\xi_{\ell,i+1} + \xi_{\ell,i+2} & \text{if } \ell = i-3, \\ \xi_{\ell,i+2} & \text{if } \ell = i-2. \end{cases} \tag{13}$$

Proof. By applying Lemma 2, we obtain

$$D^4 \rho_i = \frac{1}{16} [D^4 \bar{V}_{i-2}(x) + 4D^4 \bar{V}_{i-1}(x) + 6D^4 \bar{V}_i(x) + 4D^4 \bar{V}_{i+1}(x) + D^4 \bar{V}_{i+2}(x)]. \tag{14}$$

Finally, by applying Lemma 1 to each term on the right-hand side of (14) and collecting similar terms, the proof is completed. □

Remark 2. Consider $\rho(x) = [\rho_0(x), \rho_1(x), \rho_2(x), \dots, \rho_M(x)]^T$. Then, the fourth derivative of the vector $\rho(x)$ can be written in matrix form as

$$\frac{d^4 \rho(x)}{dx^4} = \eta \rho(x), \quad (15)$$

where $\eta = (\eta_{\ell,i})$ is the operational matrix of derivative of order $(M+1) \times (M+1)$ whose entries are given in (13).

3.2 Collocation algorithm for solving Eq. (8)

To handle Eq. (5), we approximate $u(x)$ by the Jacobi wavelets as

$$u_M(x) = \sum_{i=0}^M c_i \rho_i(x) = C^T \rho(x), \quad (16)$$

where $C^T = [c_0, c_1, c_2, \dots, c_N]$ and $\rho(x)$ are given in Remark 2.

Based on Eqs. (15) and (16), the residual of Eq. (8) is given by

$$\begin{aligned} R(x) &= \frac{d^4 u_M}{dx^4} + \alpha_K (1 + u_M)^{-K} + \mu (1 + u_M)^{-2} + \gamma (1 + u_M)^{-1} \\ &= C^T \eta \rho(x) + \alpha_K (1 + C^T \rho(x))^{-K} + \mu (1 + C^T \rho(x))^{-2} + \gamma (1 + C^T \rho(x))^{-1}. \end{aligned} \quad (17)$$

Also the boundary conditions (9) or (10) yields

$$C^T \frac{d^2 \rho(1)}{dx^2} = 0, \quad C^T \frac{d^3 \rho(1)}{dx^3} = 0, \quad (18)$$

and

$$C^T \rho(1) = 0, \quad C^T \frac{d\rho(1)}{dx} = 0. \quad (19)$$

To find the solution $u_M(x)$, we first calculate Eq. (17) at $(M-2)$ points. For a better result, we use the first $(M-2)$ roots of $\rho_{M+2}(x)$. These equations collectively with Eqs. (18) and (19) generate $(M+1)$ nonlinear equations which can be solved using Newton's iterative method. Consequently $u_M(x)$ given in Eq. (16) can be calculated.

4 The error bound

This section aims to examine the convergence of our spectral collocation method in shifted third-kind Chebyshev-weighted Sobolev spaces $\mathbf{H}_{w(x)}^m(I)$ where $I = (0, 1)$.

Consider the following generalized Chebyshev-weighted Sobolev space:

$$\mathbf{H}_{w(x)}^m(I) = \{u : u(0) = u'(0) = 0, D_x^k u \in L_{w(x)}^2(I), 0 \leq k \leq m\}, \quad (20)$$

equipped with the following inner product, norm, and semi-norm:

$$\begin{aligned} (u, v)_{\mathbf{H}_{w(x)}^m} &= \sum_{k=0}^m (D_x^k u, D_x^k v)_{L_{w(x)}^2}, \\ \|u\|_{\mathbf{H}_{w(x)}^m}^2 &= (u, u)_{\mathbf{H}_{w(x)}^m}, \quad |u|_{\mathbf{H}_{w(x)}^m} = \|D_x^m u\|_{L_{w(x)}^2}, \end{aligned} \quad (21)$$

where $m \in \mathbb{N}$.

Lemma 3 ([36]). For $n \geq 1, n+r > 1$ and $n+s > 1$, where r, s , are constants, we have the following:

$$\frac{\Gamma(n+r)}{\Gamma(n+s)} \leq \mathbf{o}_n^{r,s} n^{r-s}, \tag{22}$$

where

$$\begin{aligned} \mathbf{o}_n^{r,s} &= \exp\left(\frac{r-s}{2(n+s-1)} + \frac{1}{12(n+r-1)} + \frac{(r-s)^2}{n}\right) \\ &= 1 + O(n^{-1}). \end{aligned} \tag{23}$$

Theorem 3. Suppose $u_M(x) = \sum_{i=0}^M u_i \rho_i(x)$, is the approximate solution of $u(x) \in \mathbf{H}_{w(x)}^m(I)$. Then, for $0 \leq k \leq m \leq M+1$, we obtain the following:

$$\|D_x^k(u(x) - u_M(x))\|_{L_{w(x)}^2} \lesssim M^{-\frac{3}{4}(m-k)} \|D_x^m u(x)\|_{L_{w(x)}^2}, \tag{24}$$

where $\mathcal{X} \lesssim \mathcal{Z}$ refers to the presence of a constant n with the following: $\mathcal{X} \leq n \mathcal{Z}$.

Proof. The two expansions of $u(x)$ and $u_M(x)$ allow us to write the following:

$$D_x^k(u(x) - u_M(x)) = \sum_{n=M+1}^{\infty} u_n D_x^k G_n^{(\sigma)}(x) = \sum_{n=M+1}^{\infty} u_n \sum_{r=k}^n \frac{A_{r,n} \Gamma(r+1)}{\Gamma(r-k+1)} x^{r-k}. \tag{25}$$

Taking $\|\cdot\|_{L_{w(x)}^2}^2$, for each side of the previous equation, we obtain the following:

$$\|D_x^k(u(x) - u_M(x))\|_{L_{w(x)}^2}^2 = \sum_{n=M+1}^{\infty} |u_n|^2 \sum_{r=k}^n \frac{\sqrt{\pi} (A_{r,n})^2 \Gamma^2(r+1) \Gamma(2(r-k) - \frac{5}{2})}{\Gamma^2(r-k+1) \Gamma(2(r-k-1))}. \tag{26}$$

Also, we can write the following:

$$\|D_x^m u(x)\|_{L_{w(x)}^2}^2 = \sum_{n=m}^{\infty} |u_n|^2 \sum_{r=m}^n \frac{\sqrt{\pi} (A_{r,n})^2 \Gamma^2(r+1) \Gamma(2(r-m) - \frac{5}{2})}{\Gamma^2(r-m+1) \Gamma(2(r-m-1))}. \tag{27}$$

Now, Eq. (26) can be rewritten as follows:

$$\begin{aligned} \|D_x^k(u(x) - u_M(x))\|_{L_{w(x)}^2}^2 &= \sum_{n=M+1}^{\infty} |u_n|^2 \frac{\sum_{r=k}^n \frac{\sqrt{\pi} (A_{r,n})^2 \Gamma^2(r+1) \Gamma(2(r-k) - \frac{5}{2})}{\Gamma^2(r-k+1) \Gamma(2(r-k-1))}}{\sum_{r=m}^n \frac{\sqrt{\pi} (A_{r,n})^2 \Gamma^2(r+1) \Gamma(2(r-m) - \frac{5}{2})}{\Gamma^2(r-m+1) \Gamma(2(r-m-1))}} \\ &\quad \times \sum_{r=m}^n \frac{\sqrt{\pi} (A_{r,n})^2 \Gamma^2(r+1) \Gamma(2(r-m) - \frac{5}{2})}{\Gamma^2(r-m+1) \Gamma(2(r-m-1))}. \end{aligned} \tag{28}$$

The application of Lemma 3, enables us to write

$$\frac{\Gamma^2(r+1)}{\Gamma^2(r-k+1)} = \left(\frac{\Gamma(r+1)}{\Gamma(r-k+1)}\right)^2 \lesssim \left(r^{1-(-k+1)}\right)^2 = r^{2k}, \tag{29}$$

and

$$\frac{\Gamma(2(r-k) - \frac{5}{2})}{\Gamma(2(r-k-1))} \lesssim (2(r-k))^{-\frac{5}{2}-(-2)} \lesssim (r-k)^{-\frac{1}{2}}. \tag{30}$$

Therefore, it is possible to obtain the following inequalities:

$$\begin{aligned} \frac{\Gamma^2(r+1)\Gamma(2(r-k)-\frac{5}{2})}{\Gamma^2(r-k+1)\Gamma(2(r-k-1))} &\lesssim r^{2k}(r-k)^{-\frac{1}{2}}, \\ \frac{\Gamma^2(r+1)\Gamma(2(r-m)-\frac{5}{2})}{\Gamma^2(r-m+1)\Gamma(2(r-m-1))} &\lesssim r^{2m}(r-m)^{-\frac{1}{2}}. \end{aligned} \quad (31)$$

If we take $\phi_1^* = \max_{k \leq r \leq n} \left\{ \sqrt{\pi} (A_{r,n})^2 \right\}$, and $\phi_2^* = \max_{m \leq r \leq n} \left\{ \sqrt{\pi} (A_{r,n})^2 \right\}$, then we obtain the following:

$$\begin{aligned} \frac{\sum_{r=k}^n \frac{\sqrt{\pi} (A_{r,n})^2 \Gamma^2(r+1) \Gamma(2(r-k)-\frac{5}{2})}{\Gamma^2(r-k+1) \Gamma(2(r-k-1))}}{\sum_{r=m}^n \frac{\sqrt{\pi} (A_{r,n})^2 \Gamma^2(r+1) \Gamma(2(r-m)-\frac{5}{2})}{\Gamma^2(r-m+1) \Gamma(2(r-m-1))}} &\lesssim \frac{n^{2k} (n-k)^{-\frac{1}{2}} \phi_1^*}{n^{2m} (n-m)^{-\frac{1}{2}} \phi_2^*} \\ &\lesssim n^{2(k-m)} \left(\frac{n-k}{n-m} \right)^{-\frac{1}{2}}. \end{aligned} \quad (32)$$

The following inequality holds for $0 \leq k \leq m \leq n$:

$$\left(\frac{n-k}{n-m} \right)^{-\frac{1}{2}} = \left(\frac{\Gamma(n-k+1)\Gamma(n-m)}{\Gamma(n-k)\Gamma(n-m+1)} \right)^{-\frac{1}{2}} \leq \left(\frac{\Gamma(n-m+2)}{\Gamma(n-k+2)} \right)^{-\frac{1}{2}}. \quad (33)$$

Again, using Lemma 3, we get

$$\left(\frac{n-k}{n-m} \right)^{-\frac{1}{2}} \leq \left(\frac{\Gamma(n-m+2)}{\Gamma(n-k+2)} \right)^{-\frac{1}{2}} \lesssim n^{-\frac{1}{2}(k-m)}, \quad (34)$$

therefore, (32) gives the following:

$$\frac{\sum_{r=k}^n \frac{\sqrt{\pi} (A_{r,n})^2 \Gamma^2(r+1) \Gamma(2(r-k)-\frac{5}{2})}{\Gamma^2(r-k+1) \Gamma(2(r-k-1))}}{\sum_{r=m}^n \frac{\sqrt{\pi} (A_{r,n})^2 \Gamma^2(r+1) \Gamma(2(r-m)-\frac{5}{2})}{\Gamma^2(r-m+1) \Gamma(2(r-m-1))}} \lesssim n^{\frac{3}{2}(k-m)}. \quad (35)$$

Inserting (35) into (28) yields the following:

$$\begin{aligned} \|D_x^k(u(x) - u_M(x))\|_{L_{w(x)}^2}^2 &\lesssim (M+1)^{-\frac{3}{2}(m-k)} \sum_{n=m}^{\infty} |u_n|^2 \\ &\quad \times \sum_{r=m}^n \frac{\sqrt{\pi} (A_{r,n})^2 \Gamma^2(r+1) \Gamma(2(r-m)-\frac{5}{2})}{\Gamma^2(r-m+1) \Gamma(2(r-m-1))} \\ &= (M+1)^{-\frac{3}{2}(m-k)} \|D_x^m u(x)\|_{L_{w(x)}^2}^2 \\ &= \left(\frac{\Gamma(M+2)}{\Gamma(M+1)} \right)^{-\frac{3}{2}(m-k)} \|D_x^m u(x)\|_{L_{w(x)}^2}^2 \\ &\lesssim M^{-\frac{3}{2}(m-k)} \|D_x^m u(x)\|_{L_{w(x)}^2}^2. \end{aligned} \quad (36)$$

Therefore, we get the following result

$$\|D_x^k(u(x) - u_M(x))\|_{L_{w(x)}^2} \lesssim M^{-\frac{3}{4}(m-k)} \|D_x^m u(x)\|_{L_{w(x)}^2}. \quad (37)$$

□

5 Illustrative examples

In this section we present some numerical examples of the nonlinear electrostatic two cantilever NEMS models. Due to the non-existence of the exact solution for (5), we instead consider the following error remainder function

$$RE = \left| \frac{d^4 u_M}{dx^4} + \frac{\alpha_K}{(1+u_M)^K} + \frac{\mu}{(1+u_M)^2} + \frac{\gamma}{1+u_M} \right|, \quad (38)$$

5.1 For Eq. (8) subject to $u(1) = 0$ and $u'(1) = 0$.

In this subsection, we solved Eq. (8) for the two cases corresponding to $(k = 3, \alpha_k = 0.2, \beta = 0.5, \gamma = 0.25)$, and $(k = 4, \alpha_k = 1, \beta = 1.5, \gamma = 0.5)$.

- At $k = 3, \alpha_k = 0.2, \beta = 0.5, \gamma = 0.25$.

Table 1 presents the approximate solution and RE at $M = 18$. Figure 1 shows the Log10 RE at different values of M . Figure 2 shows the approximate solution (left) and RE (right) at $M = 18$. Figure 3 shows the RE at different values of M .

- At $k = 4, \alpha_k = 1, \beta = 1.5, \gamma = 0.5$.

Table 2 presents the approximate solution and RE at $M = 20$. Table 3 presents a comparison between present method at $M = 21$ and method in [15] at $m = 7$. Figure 4 shows the approximate solution (left) and RE (right) at $M = 21$. Table 4 shows the MRE at different values of M . Figure 2 shows the approximate solution (left) and RE (right) at $M = 18$. Figure 5 shows the RE at different values of M .

Table 1: The approximate solution and RE at $M = 18$

x	Approximate solution	RE
0	1	0
0.1	0.999678	2.22045×10^{-16}
0.2	0.998983	0
0.3	0.998248	3.33067×10^{-16}
0.4	0.997711	2.22045×10^{-16}
0.58	0.997517	1.11022×10^{-16}
0.6	0.997711	4.44089×10^{-16}
0.7	0.998248	3.33067×10^{-16}
0.8	0.998983	1.54321×10^{-14}
0.9	0.999678	5.84532×10^{-13}
1	1	2.29453×10^{-10}

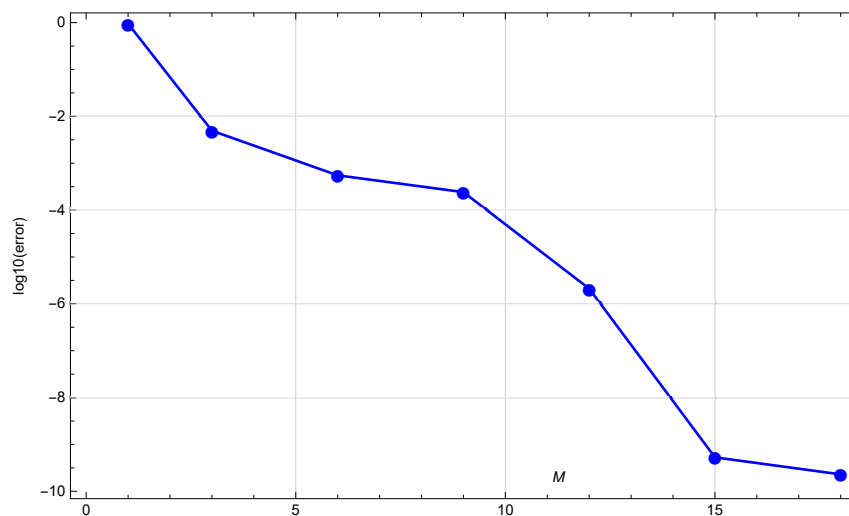


Figure 1: The Log10 RE at different values of M .

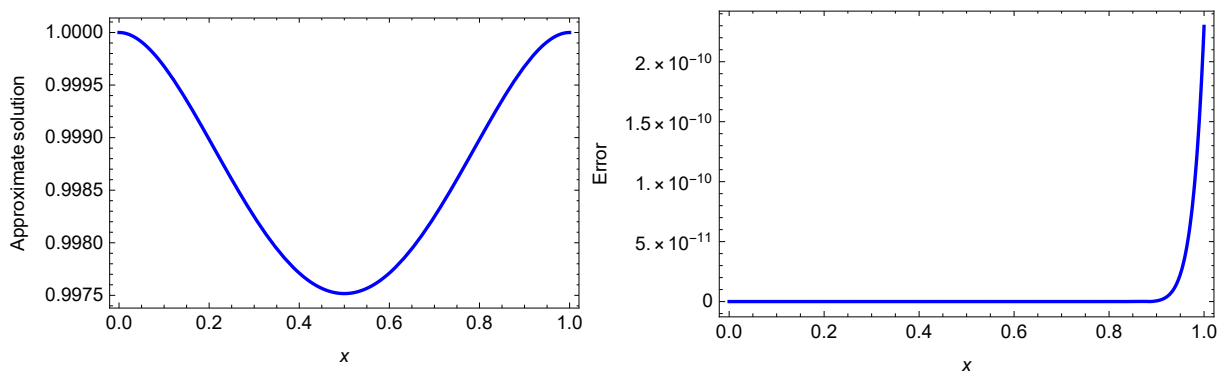


Figure 2: The approximate solution (left) and RE (right) at $M = 18$.

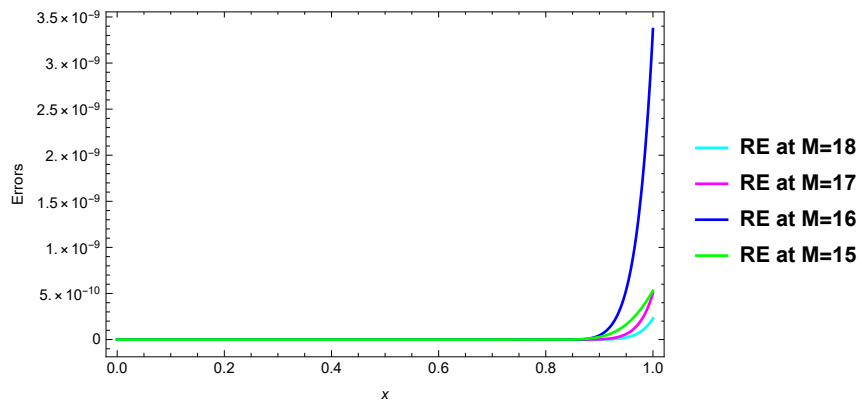


Figure 3: The RE at different values of M .

Table 2: The approximate solution and RE at $M = 20$

x	Approximate solution	RE
0	1	8.88178×10^{-16}
0.1	0.998973	0
0.2	0.996752	8.88178×10^{-16}
0.3	0.994403	1.33227×10^{-15}
0.4	0.992688	1.33227×10^{-15}
0.58	0.992066	2.66454×10^{-15}
0.6	0.992688	7.10543×10^{-15}
0.7	0.994403	2.62013×10^{-14}
0.8	0.996752	1.87406×10^{-13}
0.9	0.998973	3.27116×10^{-12}
1	1	8.39551×10^{-9}

Table 3: Comparison of the MRE

Method in [15] at $m = 7$	Present method at $M = 21$
4.9544×10^{-9}	1.0509×10^{-9}

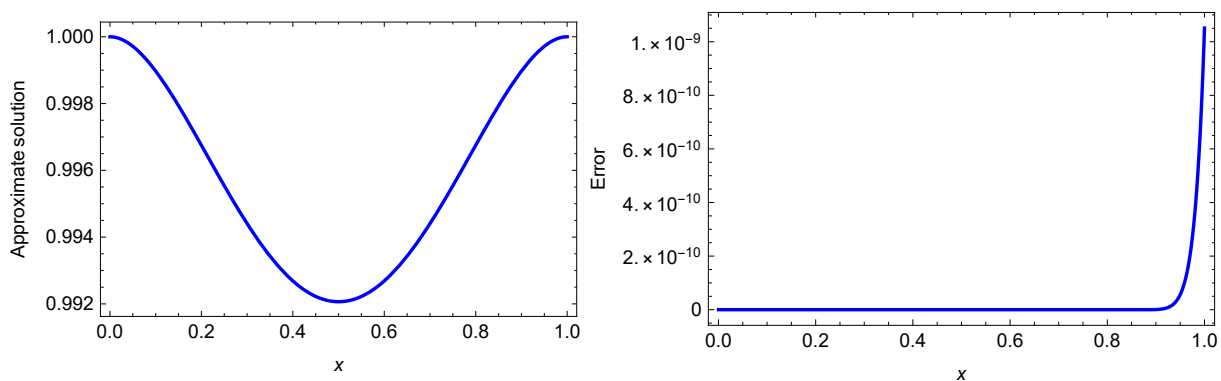


Figure 4: The approximate solution (left) and RE (right) at $M = 21$.

Table 4: The MRE at different values of M .

M	3	6	9	12	15	18	21
Error	6.371×10^{-2}	2.875×10^{-2}	1.174×10^{-2}	4.453×10^{-4}	5.045×10^{-7}	7.950×10^{-8}	1.050×10^{-9}

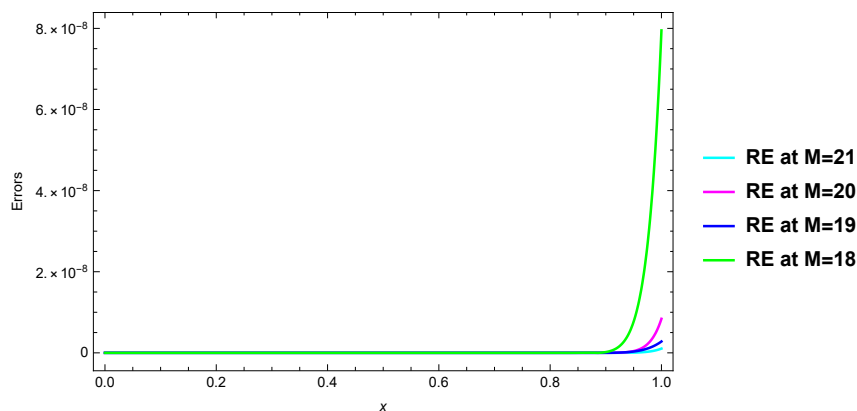


Figure 5: The RE at different values of M .

Remark 3. The approximate solution for Subsection 5.1 when $M = 18$ at $k = 3$, $\alpha_k = 0.2$, $\beta = 0.5$ and $\gamma = 0.25$, is

$$\begin{aligned}
 & 1 - 1.5659765921993467 \times 10^{-11} x^{20} + 3.8971521085054654 \times 10^{-10} x^{19} - 2.431321852134578 \times 10^{-9} x^{18} \\
 & + 7.3426502074417404 \times 10^{-9} x^{17} - 1.8986342143074385 \times 10^{-8} x^{16} + 6.342484809348224 \times 10^{-8} x^{15} \\
 & - 1.7878672898636552 \times 10^{-7} x^{14} + 3.1868773933511017 \times 10^{-7} x^{13} - 7.343568327531095 \times 10^{-7} x^{12} \\
 & + 2.5819080497396187 \times 10^{-6} x^{11} - 5.655192789752283 \times 10^{-6} x^{10} + 6.150153221294683 \times 10^{-6} x^9 \\
 & - 0.0000463584 x^8 + 0.000174806 x^7 - 0.000204091 x^6 - 7.788190705945334 \times 10^{-16} x^5 \\
 & - 0.0395833 x^4 + 0.0793715 x^3 - 0.039715 x^2.
 \end{aligned}
 \tag{39}$$

Remark 4. The approximate solution for Subsection 5.1 when $M = 21$ at $k = 4$, $\alpha_k = 1$, $\beta = 1.5$ and $\gamma = 0.5$, is

$$\begin{aligned}
 & 1 + 1.6079706451411437 \times 10^{-8} x^{23} - 1.479975280206632 \times 10^{-7} x^{22} + 5.975805450411093 \times 10^{-67} x^{21} \\
 & - 1.4599719340827782 \times 10^{-6} x^{20} + 2.8229567629231393 \times 10^{-6} x^{19} - 5.6478480471968545 \times 10^{-6} x^{18} \\
 & + 0.0000110912 x^{17} - 0.0000182073 x^{16} + 0.0000278525 x^{15} - 0.0000463653 x^{14} + 0.0000685921 x^{13} \\
 & - 0.0000894191 x^{12} + 0.000162482 x^{11} - 0.000298928 x^{10} + 0.000317655 x^9 - 0.000701415 x^8 \\
 & + 0.00225604 x^7 - 0.00264004 x^6 + 5.605487359150118 \times 10^{-16} x^5 - 0.125 x^4 + 0.252676 x^3 - 0.126722 x^2.
 \end{aligned}
 \tag{40}$$

5.2 For Eq. (8) subject to $u''(1) = 0$ and $u'''(1) = 0$.

In this subsection, we solved Eq. (8) at $k = 3$, $\alpha_k = 0.2$, $\beta = 0.5$, $\gamma = 0.25$.

- Table 5 presents a comparison between present method at $M = 21$ and method in [15] at $m = 15$ and $c = 0.1$. Figure 6 shows the Log10 RE at different values of M . Table 6 presents the MRE at different values of M . Figure 7 shows the RE at different values of M .

Table 5: Comparison of the MRE

Method in [15] at $m = 15$ and $c = 0.1$	Present method at $M = 21$
6.95319×10^{-10}	3.29736×10^{-14}

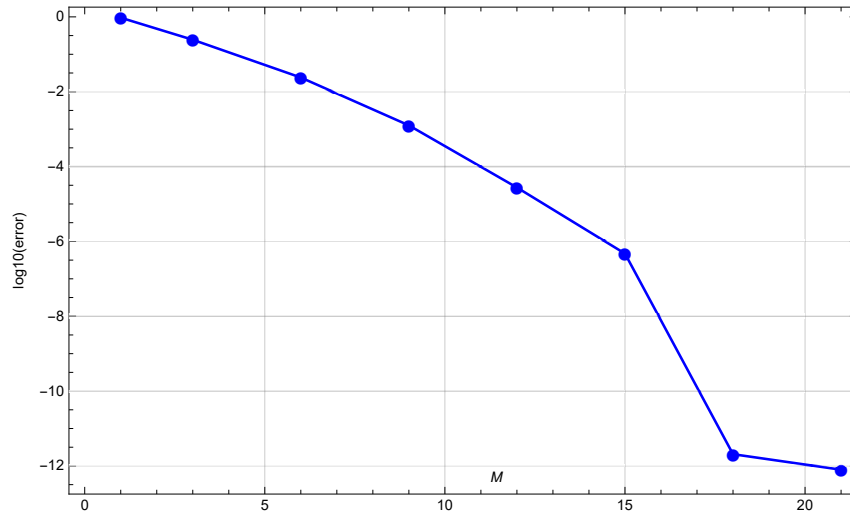


Figure 6: The Log10 RE at different values of M .

Table 6: The MRE at different values of M .

M	3	6	9	12	15	18	21
Error	2.445×10^{-1}	2.393×10^{-2}	1.259×10^{-3}	2.753×10^{-5}	4.726×10^{-7}	2.057×10^{-12}	3.297×10^{-14}

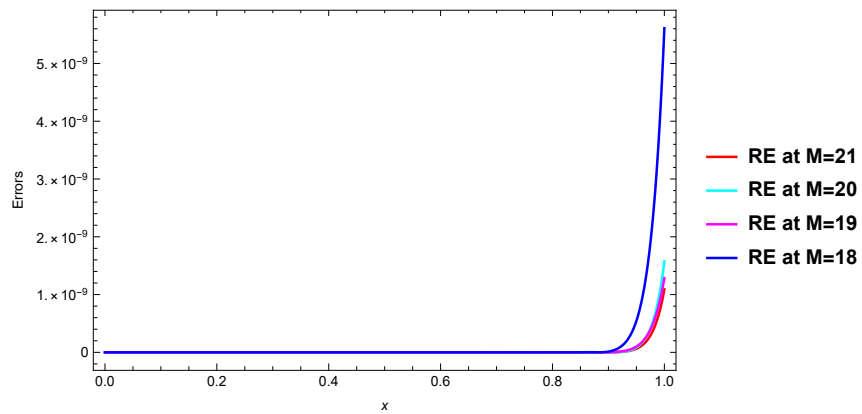


Figure 7: The RE at different values of M .

Remark 5. The approximate solution for Subsection 5.2 when $M = 18$ at $k = 3$, $\alpha_k = 0.2$, $\beta = 0.5$ and $\gamma = 0.25$,

is

$$\begin{aligned}
& 1 - 5.957731336844295 \times 10^{-9} x^{20} + 5.6533482458763184 \times 10^{-9} x^{19} - 2.594362219609357 \times 10^{-7} x^{18} \\
& + 7.798057975274253 \times 10^{-7} x^{17} - 1.7807224618780917 \times 10^{-6} x^{16} + 3.417879959338085 \times 10^{-7} x^{15} \\
& - 5.942351121011907 \times 10^{-6} x^{14} + 9.959742509498036 \times 10^{-6} x^{13} - 0.0000169516x^{12} + 0.0000286284x^{11} \\
& - 0.0000517886x^{10} + 0.0000993004x^9 - 0.000185052x^8 + 0.00039492x^7 - 0.00145859x^6 \\
& - 8.709258408722128 \times 10^{-16} x^5 - 0.0395833x^4 + 0.179315x^3 - 0.283834x^2.
\end{aligned}
\tag{41}$$

6 Closing Remarks

We presented a new third-kind Chebyshev collocation technique to solve nonlinear BVPs related to MEMS/NEMS actuator models. An effective and precise spectral approximation of the governing equations was made possible by the employment of shifted third-kind Chebyshev polynomials. The usefulness of the suggested method was validated by numerical results, which showed that it was more accurate and computationally efficient than the previous methods. In order to improve robustness, future research may investigate applying this approach to multidimensional MEMS/NEMS challenges and integrating adaptive spectrum approaches. All codes were written and debugged by *Mathematica* 11 on HP Z420 Workstation, Processor: Intel (R) Xeon(R) CPU E5-1620 v2 - 3.70GHz, 16 GB Ram DDR3, and 512 GB storage.

References

- [1] W.M. Abd-Elhameed, M.A. Bassuony, E.H. Doha, *On the coefficients of differentiated expansions and derivatives of Chebyshev polynomials of the third and fourth kinds*, *Acta Math. Sci.* **35** (2015) 326–338.
- [2] W.M. Abd-Elhameed, Y.H. Youssri, A.G. Atta, *Adopted spectral tau approach for the time-fractional diffusion equation via seventh-kind Chebyshev polynomials*, *Bound. Value Probl.* **2024** (2024) 102.
- [3] W.M. Abd-Elhameed, M.M. Alsuyuti, *New spectral algorithm for fractional delay pantograph equation using certain orthogonal generalized Chebyshev polynomials*, *Commun. Nonlinear Sci. Numer. Simul.* **141** (2025) 108479.
- [4] W.M. Abd-Elhameed, O.M. Alqubori, A.A. Alluhaybi, A.K. Amin, *Novel expressions for certain generalized Leonardo polynomials and their associated numbers*, *Axioms* **14** (2025) 286.
- [5] W.M. Abd-Elhameed, Y.H. Youssri, A.G. Atta, *Tau algorithm for fractional delay differential equations utilizing seventh-kind Chebyshev polynomials*, *J. Math. Model.* **12** (2024) 277–299.
- [6] H.M. Ahmed, W.M. Abd-Elhameed, *Spectral solutions of specific singular differential equations using a unified spectral Galerkin-collocation algorithm*, *J. Nonlinear Math. Phys.* **31** (2024) 42.
- [7] A.G. Atta, Y.H. Youssri, *Shifted second-kind Chebyshev spectral collocation-based technique for time-fractional KdV-Burgers' equation*, *Iranian J. Math. Chem.* **14** (2023) 207–224.
- [8] A.G. Atta, J.F. Soliman, E.W. Elsaed, M.W. Elsaed, Y.H. Youssri, *Spectral collocation algorithm for the fractional Bratu equation via hexic shifted Chebyshev polynomials*, *Comput. Methods Differ. Equ.*, In Press, 2024, <https://doi.org/10.22034/cmde.2024.61045.2621>.
- [9] A.G. Atta, *Approximate Petrov–Galerkin solution for the time fractional diffusion wave equation*, *Math. Methods Appl. Sci.*, In Press, 2025.

- [10] C. Bernardi, Y. Maday, *Spectral methods*, Handb. Numer. Anal. **5** (1997) 209–485.
- [11] N. Brisebarre, M. Joldeş, *Chebyshev interpolation polynomial-based tools for rigorous computing*, Proc. 2010 Int. Symp. Symbolic Algebraic Comput. (2010) 147–154.
- [12] C. Canuto, M.Y. Hussaini, A. Quarteroni, T.A. Zang, *Spectral Methods*, vol. **285**, Springer, 2006.
- [13] F. Cheli, G. Diana, *Advanced Dynamics of Mechanical Systems*, vol. **2020**, Springer, 2015.
- [14] C.W. Clenshaw, *The numerical solution of linear differential equations in Chebyshev series*, Math. Proc. Camb. Philos. Soc. **53** (1957) 134–149.
- [15] J.S. Duan, R. Rach, A. Wazwaz, *Solution of the model of beam-type micro- and nano-scale electrostatic actuators by a new modified Adomian decomposition method for nonlinear boundary value problems*, Int. J. Non-Linear Mech. **49** (2013) 159–169.
- [16] T. Fang, X.L. Leng, C.Q. Song, *Chebyshev polynomial approximation for dynamical response problem of random system*, J. Sound Vib. **266** (2003) 198–206.
- [17] H. Gomez, L. De Lorenzis, *The variational collocation method*, Comput. Methods Appl. Mech. Eng. **309** (2016) 152–181.
- [18] J. Gu, *Integration and performance optimization of gallium nitride barrier micro nano electromechanical systems in intelligent agricultural sensor networks*, Measurement: Sensors **2025** (2025) 101814.
- [19] R.M. Hafez, H.M. Ahmed, O.M. Alqubori, A.K. Amin, W.M. Abd-Elhameed, *Efficient spectral Galerkin and collocation approaches using telephone polynomials for solving some models of differential equations with convergence analysis*, Mathematics **13** (2025) 918.
- [20] W. Jiang, X. Gao, *Review of collocation methods and applications in solving science and engineering problems*, CMES-Comput. Model. Eng. Sci. **140** (2024).
- [21] J.C. Mason, D.C. Handscomb, *Chebyshev Polynomials*, Chapman and Hall/CRC, 2002.
- [22] M.O. Moustafa, Y.H. Youssri, A.G. Atta, *Explicit Chebyshev Petrov–Galerkin scheme for time-fractional fourth-order uniform Euler–Bernoulli pinned–pinned beam equation*, Nonlinear Eng. **12** (2023) 20220308.
- [23] T.J. Rivlin, *Chebyshev Polynomials*, Courier Dover Publications, 2020.
- [24] S.M. Sayed, A.S. Mohamed, E.M. Abo-Eldahab, Y.H. Youssri, *Spectral framework using modified shifted Chebyshev polynomials of the third-kind for numerical solutions of one- and two-dimensional hyperbolic telegraph equations*, Bound. Value Probl. **2025** (2025) 7.
- [25] J. Shen, T. Tang, L.-L. Wang, *Spectral Methods: Algorithms, Analysis and Applications*, vol. **41**, Springer, 2011.
- [26] M.A. Taama, Y.H. Youssri, *Third-kind Chebyshev spectral collocation method for solving models of two interacting biological species*, Contemp. Math. **2024** (2024) 6189–6207.
- [27] L.N. Trefethen, *Spectral Methods in MATLAB*, SIAM, 2000.
- [28] D. Xiu, J.S. Hesthaven, *High-order collocation methods for differential equations with random inputs*, SIAM J. Sci. Comput. **27** (2005) 1118–1139.
- [29] N.M. Yassin, E.H. Aly, A.G. Atta, *Novel approach by shifted Schröder polynomials for solving the fractional Bagley–Torvik equation*, Phys. Scr. **100** (2024) 015242.

- [30] Y.H. Youssri, M.I. Ismail, A.G. Atta, *Chebyshev Petrov–Galerkin procedure for the time-fractional heat equation with nonlocal conditions*, *Phys. Scr.* **99** (2023) 015251.
- [31] Y.H. Youssri, A.G. Atta, *Fejér-quadrature collocation algorithm for solving fractional integro-differential equations via Fibonacci polynomials*, *Contemp. Math.* **2024** (2024) 296–308.
- [32] Y.H. Youssri, A.G. Atta, *Modal spectral Tchebyshev Petrov–Galerkin stratagem for the time-fractional nonlinear Burgers’ equation*, *Iran. J. Numer. Anal. Optim.* **14** (2024) 172–199.
- [33] Y.H. Youssri, A.G. Atta, *Adopted Chebyshev collocation algorithm for modeling human corneal shape via the Caputo fractional derivative*, *Contemp. Math.* **6** (2025) 1223–1238.
- [34] Y.H. Youssri, A.G. Atta, *Chebyshev Petrov–Galerkin method for nonlinear time-fractional integro-differential equations with a mildly singular kernel*, *J. Appl. Math. Comput.* **2025** (2025) 1–21.
- [35] Y.H. Youssri, A.G. Atta, M.O. Moustafa, Z.Y. Abu Waar, *Explicit collocation algorithm for the nonlinear fractional Duffing equation via third-kind Chebyshev polynomials*, *Iran. J. Numer. Anal. Optim.*, In Press, 2025.
- [36] X. Zhao, L. Wang, Z. Xie, *Sharp error bounds for Jacobi expansions and Gegenbauer–Gauss quadrature of analytic functions*, *SIAM J. Numer. Anal.* **51** (2013) 1443–1469.